

Validation of basal ganglia segmentation on a 3T MRI template

Claire Haegelen, Nicolas Guizard, Pierrick Coupé, Florent Lalys, Pierre Jannin, Xavier Morandi, D. Louis Collins

► To cite this version:

Claire Haegelen, Nicolas Guizard, Pierrick Coupé, Florent Lalys, Pierre Jannin, et al.. Validation of basal ganglia segmentation on a 3T MRI template. Human Brain Mapping, Jun 2011, Quebec City, Canada. <inserm-00632521>

HAL Id: inserm-00632521

<https://www.hal.inserm.fr/inserm-00632521>

Submitted on 14 Oct 2011

HAL is a multi-disciplinary open access archive for the deposit and dissemination of scientific research documents, whether they are published or not. The documents may come from teaching and research institutions in France or abroad, or from public or private research centers.

L'archive ouverte pluridisciplinaire **HAL**, est destinée au dépôt et à la diffusion de documents scientifiques de niveau recherche, publiés ou non, émanant des établissements d'enseignement et de recherche français ou étrangers, des laboratoires publics ou privés.

Abstract for HBM

Validation of basal ganglia segmentation on a 3T MRI template

Haegelen C^{1,2}, Guizard N¹, Coupe P¹, Lalys F², Jannin P², Morandi X², Collins D.L.¹

¹ McCONNELL BRAIN IMAGING CENTRE, McGill University, Montreal, Canada

² Unit/Project VisAGeS U746, INRIA/ CNRS, UMR 6074, IRISA, Université Rennes I, Rennes, France

Introduction Subthalamic nucleus (STN) deep brain stimulation (DBS) has been demonstrated as an efficient surgical treatment in patients with Parkinson's disease suffering from severe disabilities in their motor symptoms (tremor, akinesia, rigidity) [1]. Sometimes, patients with STN DBS have secondary neuropsychological and/or psychiatric effects because the STN has a small size and a functional subdivision into motor, associative and limbic parts [8]. Therefore, targeting is an important step of the neurosurgical procedure as the DBS could induce undesirable side-effects. To improve targeting, many authors created either anatomical atlases [2,4] or multimodal databases [5-7]. They demonstrated that multimodal databases improved targeting accuracy over anatomical atlases. We presented a validation automatic segmentation of the basal ganglia based on a manual segmentation of these structures completed on a 3T MRI-template. This is the first step to increase accuracy of the targeting of DBS in order to improve the clinical outcome of DBS procedures.

Methods First, we developed a three-dimensional mono-subject template of the human brain by averaging 15 tridimensional (3D) T1 and 7 T2 MRI volumes acquired on a 3T scanner (Philips Medical Systems, Best, The Netherlands). The method to build the template was described in Lalys *et al.* [9]. We obtained high signal-to-noise average T1, T2 and T1-T2 mixing templates (Fig. 1) to improve the visualisation of small deep nuclei. Second, we manually painted slice-by-slice on the T1-T2 template 24 bilateral cerebral structures which included the caudate nucleus, putamen, lateral and medial pallidum, thalamus, hippocampus, amygdala, lateral and medial geniculate nuclei, red nucleus, substantia nigra and STN (Fig. 2). To validate the automatic template-based segmentation procedure, we painted 14 bilateral structures on the cerebral MRI of 5 patients with Parkinson's disease. The patients had 3D T1 without and with gadolinium injection and a 3D coronal T2 MRI on the same 3T machine. Each sequence was corrected for image intensity inhomogeneity [10]. The painted structures in the patients were bilaterally the putamen, thalamus, hippocampus, amygdala, substantia nigra and STN (Fig. 3). We registered the template onto the T1 sequence of each patient by linear and non-linear registration [1], and then registered the patient's T1 sequence to their T1 gadolinium-enhanced sequence with a linear registration. The labels, defined on the template, were mapped through

concatenated transformations onto the subject's T1 gadolinium-enhanced volume to achieve automatic structure segmentation. Finally, the automatic labels were then compared to the manual labels using a Dice Kappa metric.

Results The results are summarized in the table presented in Fig. 4. The median of the Dice Kappa rates were greater than 0.8 for the bilateral thalami (left 0.85, right 0.83) and the left putamen (0.81). The median of the Dice Kappa rates were between 0.7 and 0.8 for the bilateral amygdala, hippocampus and red nucleus, and for the right putamen. The median of the Dice Kappa rates were between 0.55 and 0.65 for the bilateral substantia nigra (left 0.57, right 0.59) and STN (left 0.58, right 0.62).

Conclusion Our method was efficient to validate based-MRI template segmentation. Our results showed better kappa correlation within the biggest structures except for the red nucleus which is an anatomically constant structure in the cerebral brain. In the future, the volume and position of these structures will be correlated with clinical outcomes of improvement in motor and neuropsychological scores. Our method could be improved in two ways, first, by validation on more patients, and second, by creating Parkinson's disease-specific template from patients which have more cortico-subcortical atrophy than normal subjects. Our goal is further to build on the template segmentation, a database of implanted electrodes in all the patients with movement disorders in our center.

References

1. Avants, B., Gee, J.C. (2004), 'Geodesic estimation of large deformation anatomical shape averaging and interpolation', *Neuroimage*, vol. 23 Suppl 1, pp. 139-150.
2. Bardinnet, E., Bhattacharjee, M., Dormont, D., et al. (2009), 'A three-dimensional histological atlas of the human basal ganglia. II. Atlas deformation strategy and evaluation in deep brain stimulation for Parkinson disease', *J Neurosurg*, vol. 110, pp. 208-219.
3. Benabid, A.L., Chabardes, S., Mitrofanis, J., Pollak, P. (2009), 'Deep brain stimulation of the subthalamic nucleus for the treatment of Parkinson's disease', *Lancet Neurol*, vol. 8, pp. 67-81.
4. Chakravarty, M.M., Bertrand, G., Hodge, C.P., Sadikot, A.F., Collins, D.L. (2006), 'The creation of a brain atlas for image guided neurosurgery using serial histological data', *Neuroimage*, vol. 30, pp. 359-376.
5. D'Haese, P.F., Cetinkaya, E., Konrad, P.E., Kao, C., Dawant, B. (2005), 'Computer-aided placement of deep brain stimulators: from planning to intra-operative guidance', *IEEE Trans Med Imaging*, vol. 24, pp. 1469-1478.
6. Guo, T., Finnis, K.W., Parrent, A.G., Peters, T.M. (2006), 'Visualization and navigation system development and application for stereotactic deep-brain neurosurgeries', *Comput Aided Surg*, vol. 11, pp. 231-239.
7. Guo, T., Parrent, A.G., Peters, T.M. (2007), 'Surgical targeting accuracy analysis of six methods for subthalamic nucleus deep brain stimulation', *Comput Aided Surg*, vol. 12, pp. 325-334.
8. Haegelen, C., Rouaud, T., Darnault, P., Morandi, X. (2009), 'The subthalamic nucleus is a key-structure of limbic basal ganglia functions', *Med Hypoth*, vol. 72, no. 4, pp. 421-426.
9. Lalys, F., Haegelen, C., Ferre, J.C., Ganaoui, O., Jannin, P. (2009), 'Construction and assessment of a 3T brain template', *Neuroimage*, vol. 49, pp. 345-354.
10. Sled, J.G., Zijendenbos, A.P., Evans, A.C. (1998), 'A nonparametric method for automatic correction of intensity nonuniformity in MRI data', *IEEE Trans Med Imaging*, vol. 17, no. 1, pp. 87-97.

Legends of figures

Figure 1. Coronal, sagittal and axial slices of the T1 (*above*) and the T1-T2 mixed (*below*) templates.

Figure 2. Anterior 3D view of the based-MRI template segmentation. From the midline to the left, and from caudal to cranial, we see the red nucleus (*light pink*), substantia nigra (*dark red*), the subthalamic nucleus (*white*), caudate nucleus (*pink*), thalamus (*light blue*), amygdala (*dark blue*), hippocampus (*red*), and putamen (*grey*).

Figure 3. Sagittal (*left above*), coronal (*right above*) and axial (*left below*) slices of a cerebral MRI of a patient with Parkinson's disease. We see the segmentation of the following bilateral structures: amygdala (*red and green*), hippocampus (*dark and light blue*), thalami (*pink and white*), putamen (*light purple and brown*), red nucleus (*light green and blue*), substantia nigra (*green and purple*), and subthalamic nucleus (*brown and dark red*).

Figure 4. Distribution of the median of kappa rates (in ordinates) according to eight bilateral anatomical structures (in axis).

AG, amygdala; HC, hippocampus; RN, red nucleus; SN, substantia nigra; STN, subthalamic nucleus; PUT, putamen; THAL, thalamus.

Figure 1. Coronal, sagittal and axial slices of the T1 (*above*) and the T1-T2 mixed (*below*) templates.

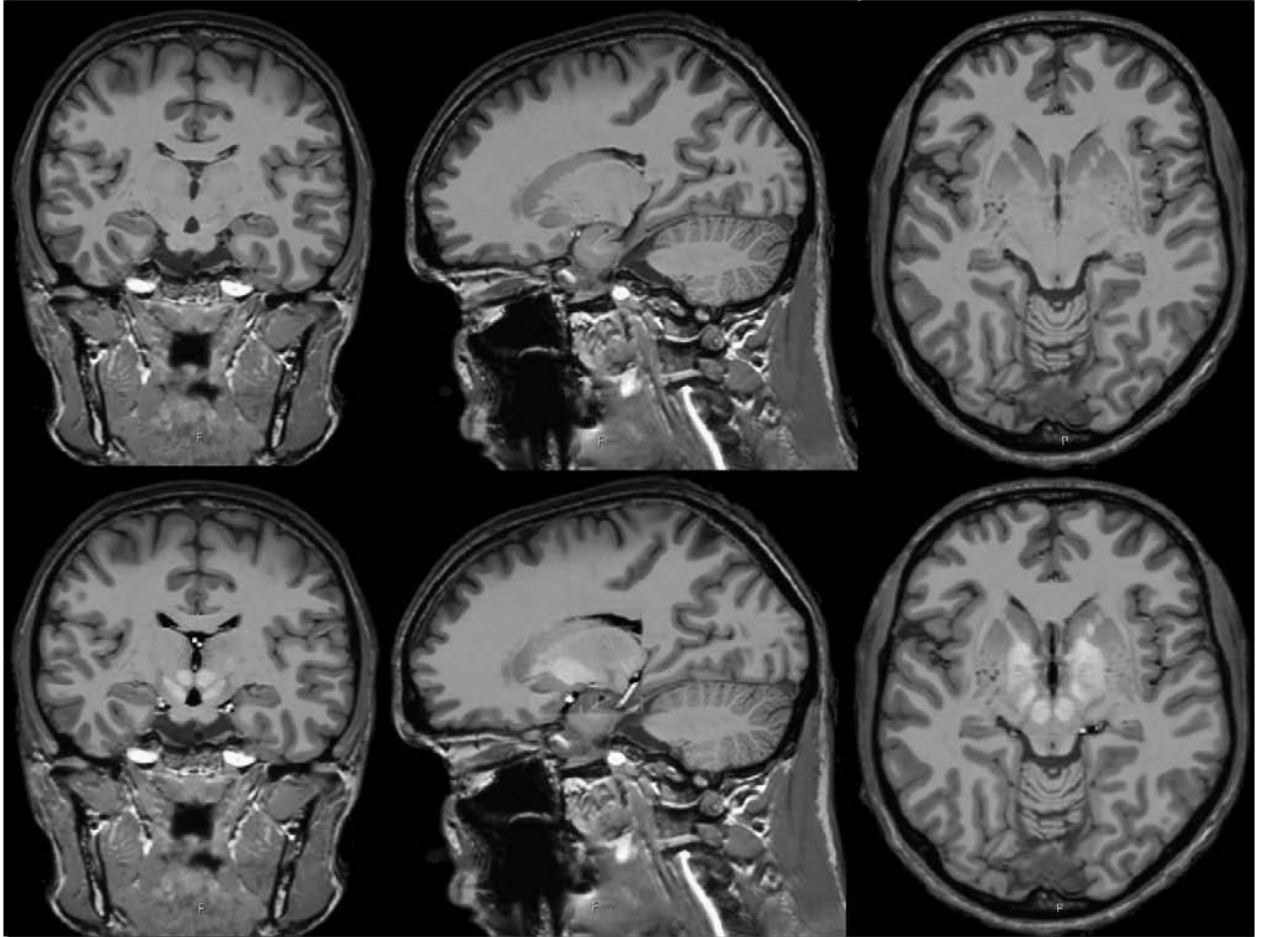


Figure 2. Anterior 3D view of the based-MRI template segmentation. From the midline to the left, and from caudal to cranial, we see the red nucleus (*light pink*), substantia nigra (*dark red*), the subthalamic nucleus (*white*), caudate nucleus (*pink*), thalamus (*light blue*), amygdala (*dark blue*), hippocampus (*red*), and putamen (*grey*).

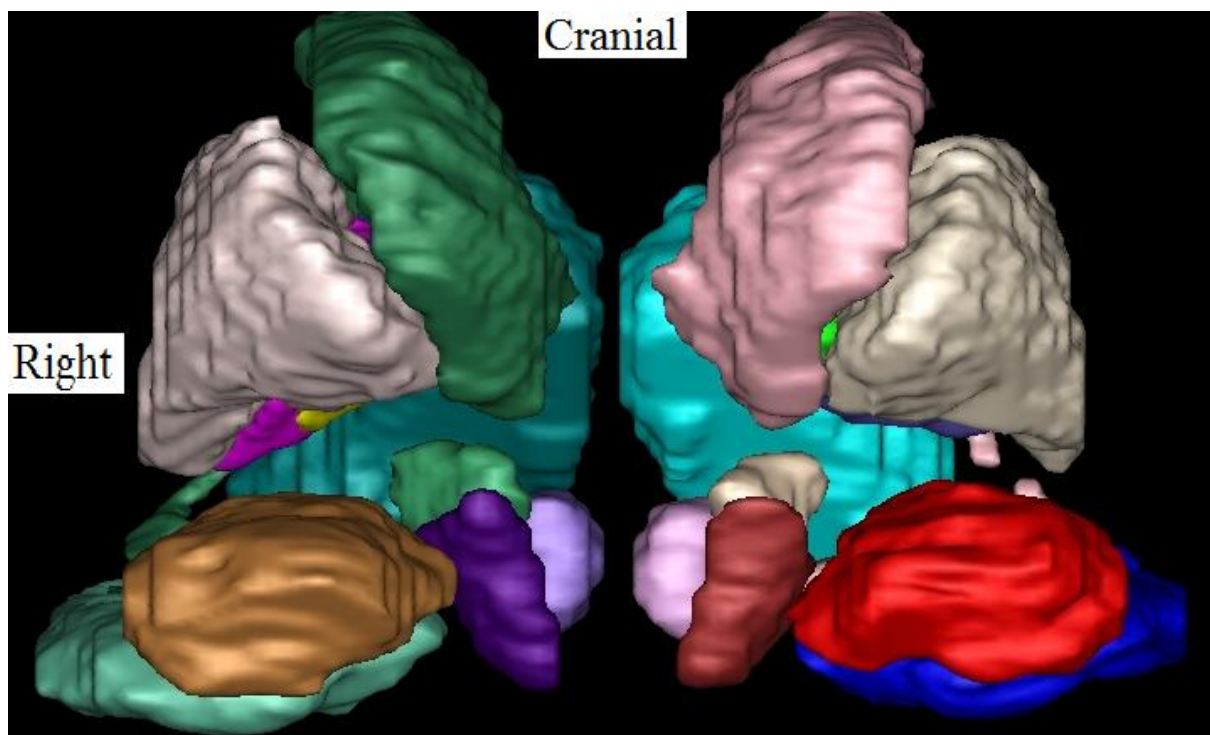


Figure 3. Sagittal (*left above*), coronal (*right above*) and axial (*left below*) slices of a cerebral MRI of a patient with Parkinson's disease. We see the segmentation of the following bilateral structures: amygdala (*red and green*), hippocampus (*dark and light blue*), thalami (*pink and white*), putamen (*light purple and brown*), red nucleus (*light green and blue*), substantia nigra (*green and purple*), and subthalamic nucleus (*brown and dark red*).

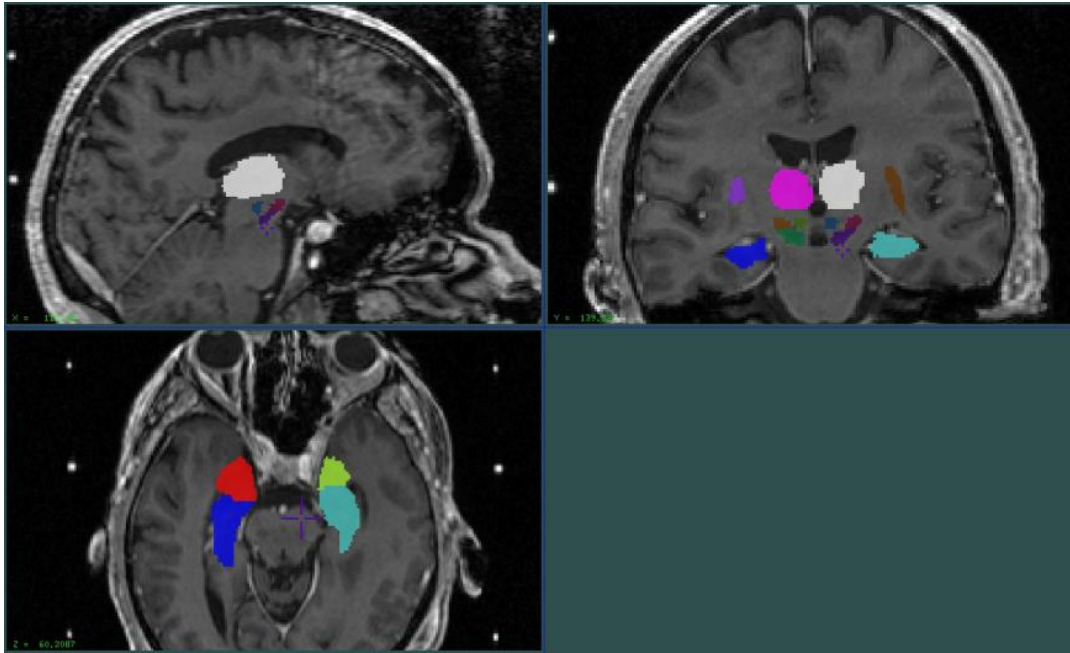


Figure 4. Distribution of the median of the Dice Kappa rates (in ordinates) according to eight bilateral anatomical structures (in axis).

AG, amygdala; HC, hippocampus; RN, red nucleus; SN, substantia nigra; STN, subthalamic nucleus; PUT, putamen; THAL, thalamus.

